Original Article
Yonsei Med J 2024 Mar;65(3):163-173
https://doi.org/10.3349/ymj.2023.0368
Yonsei Medical Journal
YMJ
pISSN: 0513-5796 · eISSN: 1976-2437

Computed Tomography Radiomics for Preoperative Prediction of Spread Through Air Spaces in the Early Stage of Surgically Resected Lung Adenocarcinomas

Young Joo Suh[1], Kyunghwa Han[1], Yonghan Kwon[2], Hwiyoung Kim[3], Suji Lee[1], Sung Ho Hwang[4], Myung Hyun Kim[5], Hyun Joo Shin[5], Chang Young Lee[6], and Hyo Sup Shim[7]

[1]Department of Radiology, Research Institute of Radiological Science, Severance Hospital, Yonsei University College of Medicine, Seoul;
[2]Department of Biostatistics and Computing, Yonsei University Graduate School, Seoul;
[3]Department of Biomedical System Informatics, Yonsei University College of Medicine, Seoul;
[4]Department of Radiology, Korea University Anam Hospital, Korea University College of Medicine, Seoul;
[5]Department of Radiology, Yongin Severance Hospital, Yonsei University College of Medicine, Yongin;
[6]Thoracic and Cardiovascular Surgery, Severance Hospital, Yonsei University College of Medicine, Seoul;
[7]Department of Pathology, Severance Hospital, Yonsei University College of Medicine, Seoul, Korea.

Purpose: To assess the added value of radiomics models from preoperative chest CT in predicting the presence of spread through air spaces (STAS) in the early stage of surgically resected lung adenocarcinomas using multiple validation datasets.

Materials and Methods: This retrospective study included 550 early-stage surgically resected lung adenocarcinomas in 521 patients, classified into training, test, internal validation, and temporal validation sets (n=211, 90, 91, and 158, respectively). Radiomics features were extracted from the segmented tumors on preoperative chest CT, and a radiomics score (Rad-score) was calculated to predict the presence of STAS. Diagnostic performance of the conventional model and the combined model, based on a combination of conventional and radiomics features, for the diagnosis of the presence of STAS were compared using the area under the curve (AUC) of the receiver operating characteristic curve.

Results: Rad-score was significantly higher in the STAS-positive group compared to the STAS-negative group in the training, test, internal, and temporal validation sets. The performance of the combined model was significantly higher than that of the conventional model in the training set {AUC: 0.784 [95% confidence interval (CI): 0.722–0.846] vs. AUC: 0.815 (95% CI: 0.759–0.872), p=0.042}. In the temporal validation set, the combined model showed a significantly higher AUC than that of the conventional model (p=0.001). The combined model showed a higher AUC than the conventional model in the test and internal validation sets, albeit with no statistical significance.

Conclusion: A quantitative CT radiomics model can assist in the non-invasive prediction of the presence of STAS in the early stage of lung adenocarcinomas.

Key Words: Lung adenocarcinoma, pathology, radiogenomics (imaging), machine learning

Received: September 11, 2023 **Revised:** October 19, 2023
Accepted: October 25, 2023 **Published online:** February 8, 2024
Corresponding author: Young Joo Suh, MD, PhD, Department of Radiology, Severance Hospital, Yonsei University College of Medicine, 50-1 Yonsei-ro, Seodaemun-gu, Seoul 03722, Korea.
E-mail: rongzu@yuhs.ac

•The authors have no potential conflicts of interest to disclose.

INTRODUCTION

Lung cancer is the leading cause of cancer-related deaths worldwide, with adenocarcinoma being the most common histologic type.[1,2] The current well-established prognostic markers of lung adenocarcinomas are patient age, pathological stage, and histologic subtype of lung adenocarcinoma.[3-6] Older age, higher pathological stage, and specific histologic subtypes, such as solid or micropapillary subtypes, are associated with worse overall and disease-free survival.

Spread through air spaces (STAS), defined as tumor cells within air spaces in the surrounding lung parenchyma beyond the edges of the main tumor, is a new negative prognostic marker for lung cancer.[7] STAS was first introduced in the 2015 World Health Organization classification of lung cancer as a new invasive pattern of adenocarcinoma.[7] STAS can predict a high risk of locoregional recurrence in lung adenocarcinomas and is closely associated with shorter recurrence-free and overall survival.[8-10] STAS also provides crucial information for determining the appropriate extent of surgical resection in the early stage of lung cancer since its presence indicates the presence of potential residual tumor cells in the surgical margins of patients who undergo limited resection, resulting in a worse prognosis than in those who undergo lobectomy.[11,12]

Despite the importance of STAS in the treatment of early-stage lung cancer, its detection is limited to preoperative sampling in small biopsied tissues. Even intraoperative frozen sections show limited accuracy, with a sensitivity, specificity, and negative predictive value of 71%, 92%, and 8%, respectively.[12-14] As a result, several studies have attempted to predict STAS preoperatively using non-invasive imaging, such as computed tomography (CT) or positron emission tomography.[15-18] However, most previous studies have focused on qualitative analysis, which could be affected by subjectivity; therefore, quantitative information would be more valuable for clinical utility.

"Radiomics," an emerging tool that provides quantitative imaging parameters, has been applied in oncology for tumor assessment and the evaluation of patient responses to treatment. Radiomics is widely applicable to lung cancer, such as in the prediction of epidermal growth factor receptor mutations and response to targeted therapy in non-small cell lung cancers.[19-23] Several previous studies have reported that quantitative radiomics features can be helpful in predicting the presence of STAS in lung cancer,[24-29] which is attributed to the ability of the radiomics approach to provide objective and quantitative parameters of the segmented regions. However, these studies have several limitations with regard to their methodology and quality of reporting,[30] such as insufficient investigation of the added value of radiomics models to conventional parameters and incomplete validation of radiomics models.

Therefore, the present study aimed to assess the added value of quantitative radiomics models from preoperative chest CT in predicting the presence of STAS in the early stages of surgically resected lung adenocarcinomas using multiple validation datasets.

MATERIALS AND METHODS

Patients

This study was approved by the Institutional Review Boards of the participating hospital (Severance Hospital; IRB No 4-2020-1231), and the requirement for informed consent was waived due to the retrospective nature of the study. This study followed the Transparent Reporting of a multivariable prediction model for Individual Prognosis Or Diagnosis guidelines, and assessment was conducted using the radiomics quality score.[30] To develop a radiomics model, we conducted a retrospective chart review and identified 450 patients who underwent surgical resection for clinical stage IA (tumor size ≤3 cm) lung adenocarcinoma according to the 8th edition of the TNM classification[4] at our institution between January 2016 and December 2017 (Fig. 1). Among these 450 patients, 87 were excluded for the following reasons: 1) unavailability of chest CT images with slice thickness ≤3 mm prior to surgery (n=76); 2) indistinguishable primary lesion in CT scan due to parenchymal collapse (n=4); and 3) patients with errors in radiomics feature extraction (n=7). Final pathological stage was not used for the exclusion. A total of 363 patients were included (168 male, mean age: 64.1±10.1 years, range: 29–85 years), and were classified as follows: 291 patients who underwent preoperative CT at our institution for development (training and testing) of the radiomics model and 72 patients who underwent preoperative CT at an outside hospital for model validation (internal validation set). Eleven patients had two tumor lesions, and 18 patients with outside chest CT scans underwent both contrast-enhanced and non-contrast scans. Therefore, 392 lesions in 363 patients were included in the final analysis. The development dataset of 301 lesions from 291 patients was randomly split into training set (211 lesions) and test set (90 lesions) at a ratio of 7:3, maintaining the proportion of STAS-positive lesions at approximately 30% for each dataset. For further validation of the radiomics model, 158 patients who underwent surgical resection for early-stage lung adenocarcinoma at our institution between January and December 2018 were included (temporal validation set). A total of 319 patients in the training, test, and internal validation sets comprised the outcome cohort for prediction of postoperative recurrence.

CT image analysis

For all patients, preoperative chest CT scans were performed within 2 weeks of lung cancer surgery. Additional details regarding CT image acquisition are provided in Supplementary Table 1 (only online).

Preoperative chest CT images were reviewed and analyzed by a board-certified thoracic radiologist with 9 years of experience in thoracic radiology who was blinded to the patients' clinical and pathological information. The lesion characteristics were assessed and classified into four categories: pure ground-glass nodule (GGN), ground-glass opacity (GGO)-dominant part-solid nodule (PSN), solid-dominant PSN, and solid nodules. The GGO portion was defined as increased opacity that did not obscure the adjacent airway and pulmonary vascular structures. The proportion of GGO was calculated according to the ratio of maximum GGO diameter to that of the total tumor across the largest cross-section, and classified as follows:

https://doi.org/10.3349/ymj.2023.0368

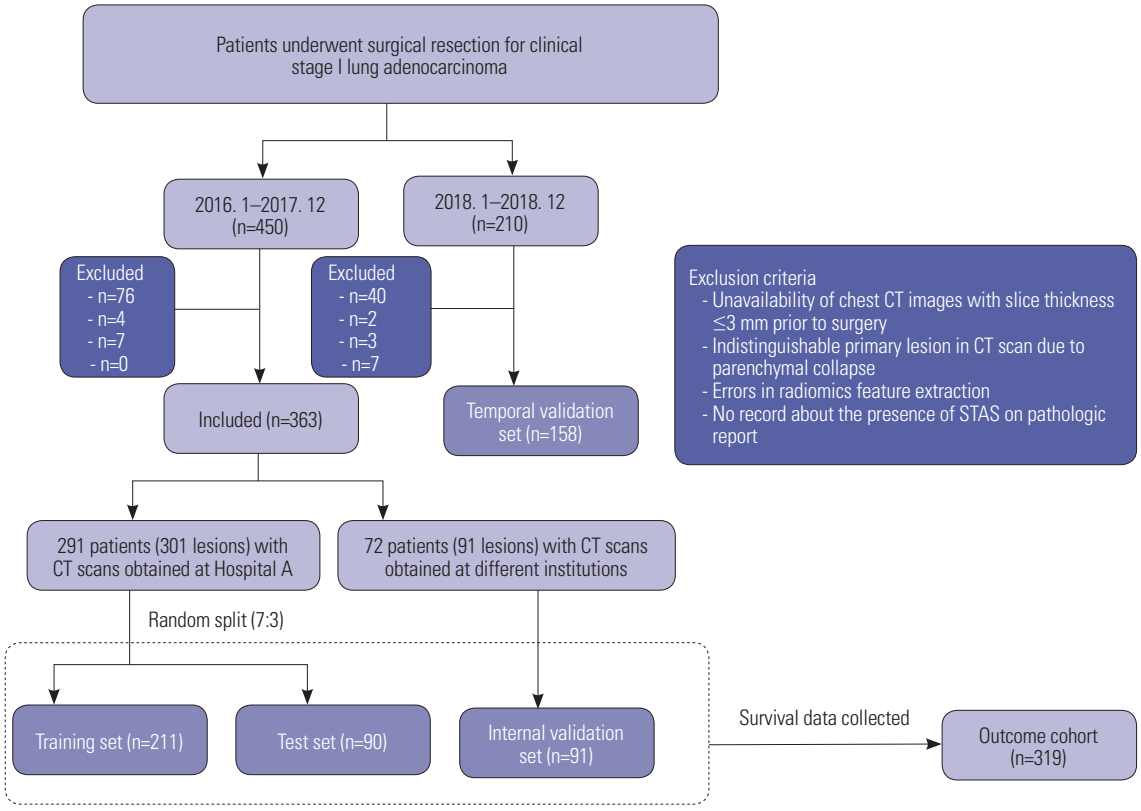

Fig. 1. Patient selection diagram. STAS, spread through air spaces.

pure GGN; GGO 100%, GGO-dominant PSN; 50%≤GGO <100%, solid-dominant PSN; 0%<GGO<50%, solid nodule; and GGO 0%.[31] The longitudinal diameter of the entire tumor was measured on CT images reconstructed with orthogonal multiplanes (axial, coronal, and sagittal) in the lung window setting (window width, 1500 HU; level, -700 HU), and the largest diameter was used as the representative diameter.[32,33] If the lesion was classified as PSN, the diameter of the inner solid portion was also measured.

CT radiomics feature extraction

A board-certified thoracic radiologist who was blinded to the patients' clinical and pathologic information performed semi-automated segmentation of the tumor lesion using a commercialized software (AVIEW Research, Coreline Soft Inc., Seoul, Korea). Lesion segmentation was performed three-dimensionally using a lung window setting (width, 1500 HU; level, -700 HU) (Fig. 2), and the volume of interest of the tumor nodule was delineated, excluding large vessels and bronchioles where possible. For interobserver agreement of segmentation, another board-certified thoracic radiologist with 2 years of experience in thoracic radiology, who was blinded to the other observer's segmentation results, independently performed segmentation for 100 cases in the training set.

The following 93 radiomics features were extracted from the nodule masks using Pyradiomics (Pyradiomics library, version 2.2.0; Computational Imaging and Bioinformatics Lab, Harvard Medical School, Boston, MA, USA)[34]: 18 histogram features, 24 gray-level co-occurrence matrix (GLCM) features, 16 gray-level run-length matrix (GLRLM) features, 16 gray-level size zone matrix (GLSZM) features, 5 neighboring gray tone difference matrix (NGTDM) features, and 14 shape features (Supplementary Table 2, only online). The processing parameters for radiomics feature extraction were based on those reported by the Image Biomarker Standardization Initiative in a previous publication (Supplementary Table 3, only online).[35]

Pathological data

Pathological data were collected from the surgical pathologic report. Tumor STAS was defined as tumor cells within the air spaces in the lung parenchyma, beyond the edge of the main tumor.[36] Pathologic subtypes were classified as lepidic, acinar, papillary, micropapillary, solid, invasive mucinous adenocarcinoma, or miscellaneous, according to the 2011 International Association for the Study of Lung Cancer/American Thoracic Society/European Respiratory Society classification of lung adenocarcinoma.[37]

Radiomics feature selection

To reduce the high dimensionality of radiomics features to the number of events, radiomics feature selection was performed using data from the training set in two sequential steps. First,

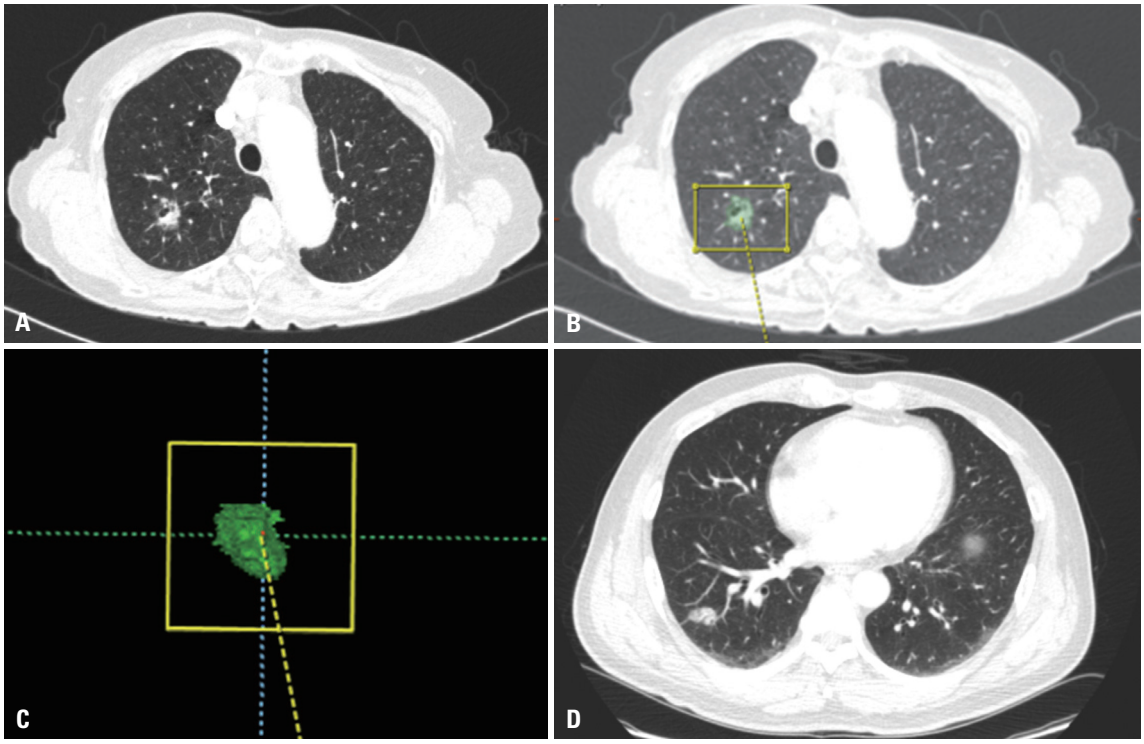

Fig. 2. Representative CT images of lung adenocarcinomas. (A) Axial CT image of an 81-year-old female showing a 22.1-mm part-solid nodule (solid portion diameter: 12.6 mm) in the right upper lobe. (B and C) Tumor segmentation was performed on the volume of interest of the right upper lobe nodule. Rad-score from the segmented ROI of the lesion: -0.718. On surgical pathology, the lesion was confirmed as a STAS-positive lung adenocarcinoma with acinar predominant histologic subtype. (D) Axial CT image of a 56-year-old male showing a 22.2-mm part-solid nodule (solid portion diameter: 19.6 mm) in the right lower lobe. Rad-score: -1.153. On surgical pathology, the lesion was confirmed as a STAS-negative lung adenocarcinoma with acinar predominant histologic subtype. ROI, region of interest; STAS, spread through air spaces.

intraclass correlation coefficients (ICC) were calculated to evaluate interobserver reproducibility, and features with poor interobserver reproducibility (ICC<0.8) were excluded from the subsequent analyses. Next, for the remaining features showing ICC≥0.8, least absolute shrinkage and selection operator (LASSO) was performed with 10-fold cross-validation to overcome the overfitting problem, and features showing nonzero coefficients using LASSO-logistic regression were selected.[38] A radiomics score (Rad-score) was calculated for each case using a linear combination of selected features that were weighted by their respective coefficients calculated using the LASSO logistic regression model.[39] ComBat harmonization was applied for the training, internal and temporal validation sets, to compensate the effect of the heterogeneity of the datasets, considering the dataset or contrast administration as a batch effect.[40,41]

Outcome prediction

Patients were divided into high- and low-score groups based on the optimal Rad-score cutoff in the outcome cohort for prediction of postoperative recurrence. The occurrence and date of postoperative recurrence were investigated until the clinical follow-up end date of February 21, 2022. Recurrence was defined as disease appearance at either intrapulmonary or extrapulmonary distant sites after at least 3 months of the disease-free interval between lung cancer surgery and recurrence. The date of recurrence was defined as the date of the first examination on which recurrence was suspected.

Statistical analysis

Statistical analyses were performed using R software (version 4.1.2., R Foundation for Statistical Computing, Vienna, Austria). Categorical variables are presented as numbers and percentages. Continuous variables are presented as the mean±standard deviation. Demographics, CT lesion type and size, and CT radiomics features were compared between the STAS-positive and STAS-negative groups using the chi-square test for categorical variables and the independent t-test for continuous variables. Interobserver agreement for CT radiomics features was analyzed using the ICC.

The diagnostic performance of clinical variables, CT lesion type/size, and Rad-score for the preoperative diagnosis of STAS were assessed using the area under the curve (AUC) of receiver operating characteristic (ROC) curves. The optimal cutoff value of the Rad-score to predict the presence of STAS was calculated from the ROC curves using the Youden index. We constructed the following three models for the diagnosis of STAS: 1) Model 1, conventional model based on clinical and conventional CT variables (CT lesion type and solid portion size);

https://doi.org/10.3349/ymj.2023.0368

https://doi.org/10.3349/ymj.2023.0368

Table 1. Patient Demographics and Lesion Characteristics

	Training set (n=211)			Test set (n=90)			Internal validation set (n=91)			Temporal validation set (n=158)		
Number of STAS positive lesions (proportion)	72 (34.1)			27 (30.0)			38 (41.8)			37 (23.4)		
Variables	**STAS negative (n=139)**	**STAS positive (n=72)**	***p* value**	**STAS negative (n=63)**	**STAS positive (n=27)**	***p* value**	**STAS negative (n=53)**	**STAS positive (n=38)**	***p* value**	**STAS negative (n=121)**	**STAS positive (n=37)**	***p* value**
Sex			0.038			0.304			0.005			0.647
Male	62 (44.6)	43 (59.7)		23 (36.5)	13 (48.1)		15 (28.3)	22 (57.9)		44 (36.4)	15 (40.5)	
Female	77 (55.4)	29 (40.3)		40 (63.5)	14 (51.9)		38 (71.7)	16 (42.1)		77 (63.6)	22 (59.5)	
Age (yr)	64.7±9.3	64.9±10.6	0.901	63.6±9.8	66.6±13.0	0.238	63.5±9.2	61.2±10.2	0.261	65.0±10.3	61.5±14.6	0.177
Location			0.227			0.192			0.201			0.752
Right upper lobe	51 (36.7)	23 (31.9)		23 (36.5)	12 (44.4)		22 (41.5)	15 (39.5)		53 (43.8)	14 (37.8)	
Right middle lobe	11 (7.9)	9 (12.5)		4 (6.3)	1 (3.7)		3 (5.7)	2 (5.3)		9 (7.4)	3 (8.1)	
Right lower lobe	20 (14.4)	10 (13.9)		21 (33.3)	3 (11.1)		5 (9.4)	9 (23.7)		21 (17.4)	8 (21.6)	
Left upper lobe	36 (25.9)	12 (16.7)		7 (11.1)	6 (22.2)		9 (17)	8 (21.1)		26 (21.5)	6 (16.2)	
Left lower lobe	21 (15.1)	18 (25.0)		8 (12.7)	5 (18.5)		14 (26.4)	4 (10.5)		12 (9.9)	6 (16.2)	
Lesion type on CT			<0.001			<0.001			<0.001			<0.001
Pure ground-glass nodule	2 (1.4)	0 (0)		3 (4.8)	0 (0)		1 (1.9)	0 (0)		0 (0)	0 (0)	
GGO-predominant part-solid nodule	70 (50.4)	6 (8.3)		27 (42.9)	1 (3.7)		19 (35.8)	1 (2.6)		59 (48.8)	6 (16.2)	
Solid-predominant part-solid nodule	50 (36.0)	32 (44.4)		28 (44.4)	9 (33.3)		26 (49.1)	12 (31.6)		56 (46.3)	9 (24.3)	
Solid nodule	17 (12.2)	34 (47.2)		5 (7.9)	17 (63.0)		7 (13.2)	25 (65.8)		6 (5.0)	22 (59.5)	
Entire tumor size on CT (mm)	18.8±6.8	18.1±6.1	0.442	18.7±7.6	21.4±5.4	0.096	22.1±6.9	20.6±5.5	0.267	18.3 [12.7; 23.2]*	20 [15.6; 25.5]*	0.374
Solid portion size on CT (mm)	9.8±6.9	14.4±6.0	<0.001	9.4±6.3	18.8±5.7	<0.001	13.5±7.2	18.6±6.4	0.007	7.9 [5.7; 13.6]*	15.8 [12.2; 19.9]*	<0.001
Histologic subtype on pathology			<0.001			<0.001			0.004			0.003
Adenocarcinoma in situ	1 (0.7)	0 (0)		1 (1.6)	0 (0)		0 (0)	0 (0)		2 (1.7)	0 (0)	
Minimally invasive adenocarcinoma	10 (7.2)	0 (0)		6 (9.5)	0 (0)		0 (0)	0 (0)		8 (6.6)	0 (0)	
Lepidic predominant	49 (35.3)	1 (1.4)		24 (38.1)	0 (0)		10 (18.9)	0 (0)		33 (27.3)	0 (0)	
Acinar predominant	61 (43.9)	44 (61.1)		26 (41.3)	16 (59.3)		35 (66.0)	21 (55.3)		58 (47.9)	25 (67.6)	
Papillary predominant	11 (7.9)	7 (9.7)		1 (1.6)	3 (11.1)		5 (9.4)	8 (21.1)		15 (12.4)	10 (27.0)	
Solid predominant	3 (2.2)	7 (9.7)		2 (3.2)	5 (18.5)		2 (3.8)	7 (18.4)		1 (0.8)	1 (2.7)	
Micropapillary predominant	0 (0)	4 (5.6)		0 (0)	1 (3.7)		0 (0)	0 (0)		0 (0)	0 (0)	
Invasive mucinous adenocarcinoma	4 (2.9)	8 (11.1)		3 (4.8)	2 (7.4)		1 (1.9)	2 (5.3)		4 (3.3)	1 (2.7)	
Miscellaneous	0 (0)	1 (1.4)		0 (0)	0 (0)		0 (0)	0 (0)		0 (0)	0 (0)	
Type of lung cancer surgery			0.716			0.332			0.393			0.212
Lobectomy	101 (72.7)	54 (75.0)		40 (63.5)	20 (74.1)		50 (94.3)	34 (89.5)		61 (50.4)	23 (62.2)	
Limited resection	38 (27.3)	18 (25.0)		23 (36.5)	7 (25.9)		3 (5.7)	4 (10.5)		60 (49.6)	14 (37.8)	

STAS, spread through air spaces; GGO, ground-glass opacity.
Data are presented as mean±standard deviation or n (%).
*Data are presented as median with interquartile range in parenthesis.

2) Model 2, radiomics model based on Rad-score; and 3) Model 3, combined model based on combinations of conventional and radiomics features (Rad-score). We compared the AUC of Model 3 (combined model) to that of Model 1 (conventional model) to investigate the added value of radiomics features in the test and validation sets. The AUC of each model for diagnosing STAS was compared using the DeLong method.[42] The calibration (goodness-of-fit) of the prediction model was assessed using the Spiegelhalter z-test and a calibration plot. The log-rank test was performed to compare the recurrence-free survival of low- and high- score group in the outcome cohort. A p-value<0.05 was considered statistically significant.

RESULTS

Clinical characteristics of patients

The clinical characteristics of patients included in the development/test datasets and validation sets (internal and temporal validation sets) are presented in Table 1. The proportion of STAS-positive lesions ranged from 23.4% to 41.8%. A higher proportion of male sex in the STAS-positive group was observed in the training set and internal validation set (p<0.05), while there was no significant difference in age between the STAS-positive and STAS-negative groups in any of the datasets (p>0.05). Regarding the lesion type, the STAS-positive group tended to show a higher proportion of solid predominant PSN or solid nodules and a larger solid portion size on preoperative CT (p<0.05). The acinar histologic subtype was most frequent in both the STAS-positive and STAS-negative groups, but the frequency of solid or micropapillary subtype was higher in the STAS-positive group in all datasets (p<0.05). The type of lung cancer surgery (lobectomy vs. limited resection) was not different between the STAS-positive and STAS-negative groups in any of the datasets (p>0.05).

Selection of CT radiomics features

Most of the radiomics features in the training set showed good-to-excellent interobserver agreement (ICC ≥0.8). The details of the ICCs for all radiomics features are described in Supplementary Table 2 (only online). Three features with an ICC<0.8 (firstorder_Energy, firstorder_TotalEnergy, and ngtdm_Busyness) were excluded from the sequential feature selection step. Among the remaining 90 radiomics features, 45 showed a significant difference between STAS-positive and STAS-negative groups in the training dataset (p<0.05) (Supplementary Table 4, only online).

Calculation and cutoff analysis for Rad-score

LASSO was performed for 90 features showing ICC ≥0.8. After radiomics feature selection using LASSO, two radiomics features (firstorder _Mean and glcm_Maximum Probability) were selected (Table 2) and the radiomics signature was computed as a Rad-score using the following formula:

Rad-score=firstorder_Mean×0.00214080251828777+glcm_MaximumProbability×0.30988439802307

Table 2. Comparison of Rad-Score According to the Presence of STAS

Dataset	STAS negative	STAS positive	*p* value
Train (n=211)	-0.820±0.426 (n=139)	-0.445±0.489 (n=72)	<0.001
Test (n=90)	-0.746±0.346 (n=63)	-0.330±0.480 (n=27)	<0.001
Internal validation (n=91)	-0.668±0.335 (n=53)	-0.286±0.350 (n=38)	<0.001
Temporal validation (n=158)	-0.815±0.351 (n=121)	-0.237±0.353 (n=37)	<0.001

STAS, spread through air spaces.

Rad-score was significantly higher in the STAS positive group than in the STAS negative group in the training set (–0.445±0.489 vs. -0.820±0.426, p<0.001) (Table 2), test set, and internal and temporal validation sets (p<0.05). Results of cutoff analysis of Rad-score are presented in Supplementary Table 5 (only online). The Rad-score of lepidic predominant histologic subtype tumors was significantly lower than that of acinar/papillary or solid/micropapillary subtype tumors (-0.992±0.286 vs. -0.562±0.426 vs. -0.406±0.500; p<0.05).

Diagnostic model for the presence of STAS

Model 1 (conventional model) was built based on three clinical or conventional CT parameters (sex, lesion type, and solid portion size on CT), which showed a significant difference between the STAS-positive and STAS-negative groups in the training set. Among the three established diagnostic models for the presence of STAS, the performance of Model 3 (combined model) was significantly better than that of Model 1 (conventional model) in the training set {AUC: 0.784 [95% confidence interval (CI): 0.722–0.846] for Model 1 vs. AUC: 0.815 (95% CI: 0.759–0.872) for Model 3; p<0.05} (Table 3 and Fig. 3). In the test and internal validation sets, Model 3 (combined model) showed a higher AUC compared to Model 1, albeit with no statistical significance. In the temporal validation sets, Model 3 showed significantly higher AUC compared to Model 1 [AUC: 0.834 (95% CI: 0.755–0.912) for Model 3, p=0.001]. The AUC of the diagnostic models in each dataset remained similar after applying the combat method (Supplementary Table 6, only online).

Calibration and radiomics quality score

All models showed good calibration except for Models 1 and 2 in the temporal validation set [Supplementary Fig. 1 (only online) and Supplementary Table 7 (only online)]. The radiomics quality score of this study was 47.2% (17 of 36).

Outcome prediction of Rad-score

The median follow-up duration was 1679 days (interquartile range: 1452.8–1822 days). Among the 319 patients in the out-

https://doi.org/10.3349/ymj.2023.0368

come cohort, 26 (8.2%) experienced postoperative recurrence of lung cancer [13.2% (22 of 167) in the high Rad-score group and 2.6% (4 of 152) in the low Rad-score group], and the high Rad-score group was associated with worse recurrence-free survival (p<0.001) (Fig. 4) with 5-year recurrence free survival of 97.3% for the high Rad-score group and 86.4% for in the low Rad-score group.

Table 3. Diagnostic Performance of Clinical and Radiomics Models for the Presence of STAS

	Number of selected features	Name of selected features	Train (n=211)	Test (n=90)	Internal validation (n=91)	Temporal validation (n=158)
Model 1: Conventional model (clinical parameter+ CT variables)	3	Lesion type on CT, solid portion size on CT, male sex	0.784 (0.722, 0.846)	0.814 (0.72, 0.907)	0.854 (0.776, 0.932)	0.742 (0.629, 0.855)
Model 2: Radiomics model	2	firstorder_Mean, glcm_ MaximumProbability	0.731 (0.657, 0.806)	0.77 (0.651, 0.888)	0.792 (0.697, 0.888)	0.869 (0.804, 0.933)*
Model 3: Combined model	5	Lesion type on CT, solid portion size on CT, male sex, firstorder_Mean, glcm_ MaximumProbability	0.815 (0.759, 0.872)*	0.859 (0.779, 0.939)	0.878 (0.808, 0.949)	0.834 (0.755, 0.912)*

STAS, spread through air spaces; CT, computed tomography; AUC, area under the curve.
*Statistical significance for comparison with the AUC of Model 1.

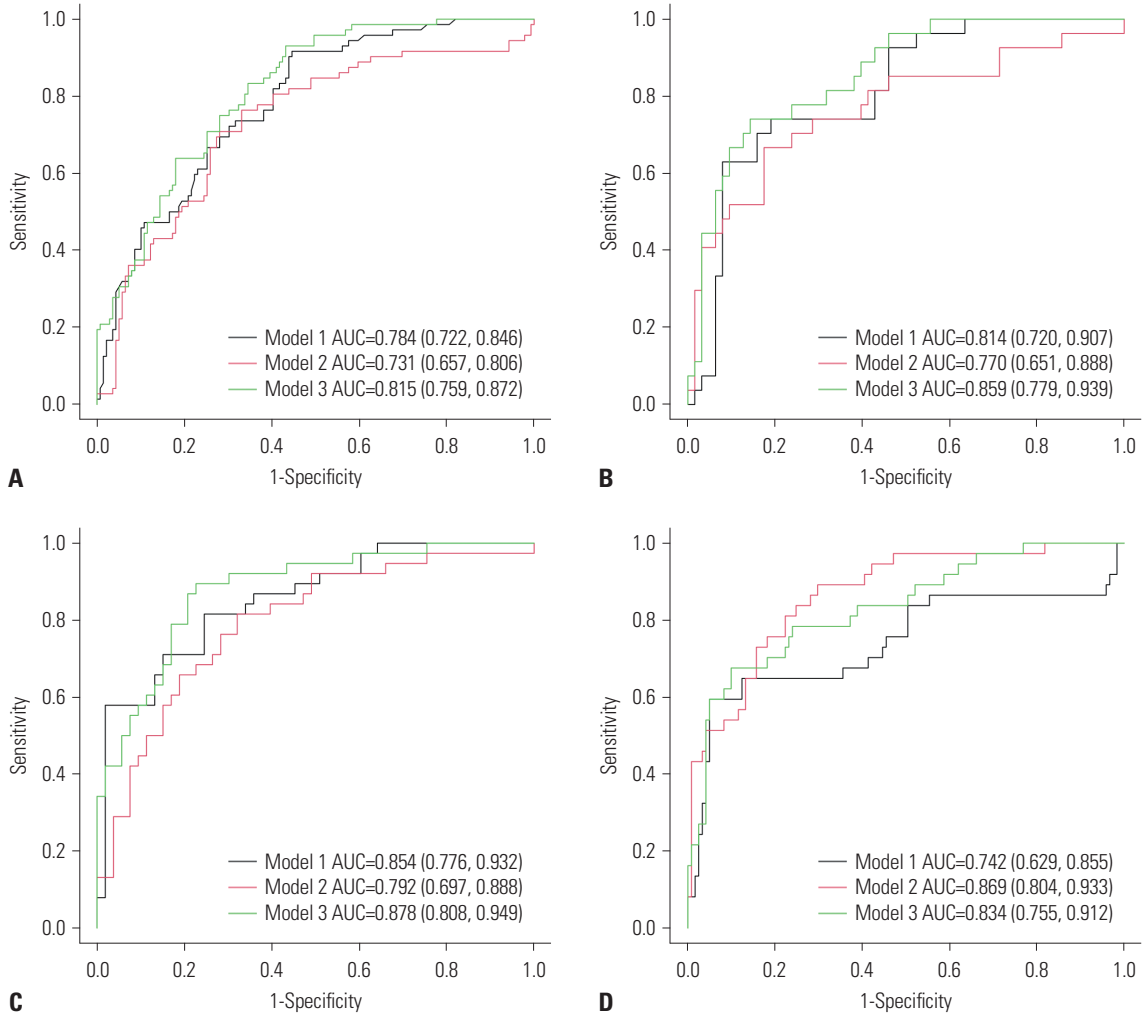

Fig. 3. ROC curves of prediction models (Model 1, conventional model; Model 2, radiomics model; Model 3, combined model) for the presence of STAS in the (A) training set, (B) test set, (C) internal validation set, and (D) temporal validation set. ROC, receiver operating characteristic; STAS, spread through air spaces; AUC, area under the curve.

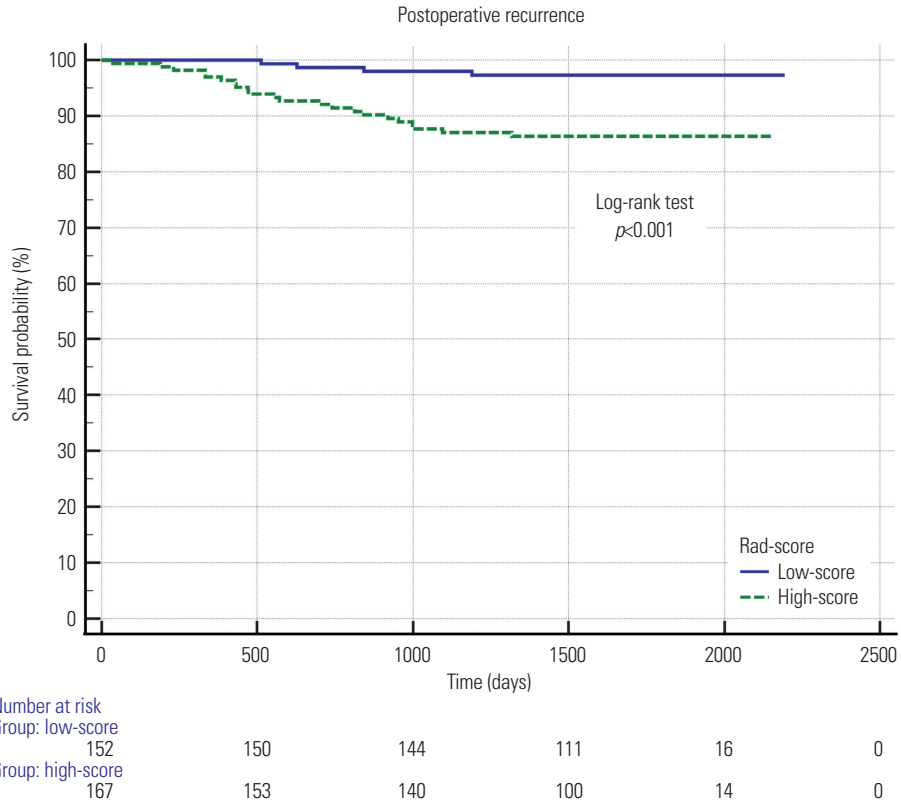

Fig. 4. Kaplan–Meier curve demonstrating the recurrence-free survival of the high and low Rad-score groups in the outcome cohort.

DISCUSSION

Our study demonstrated that the quantitative CT radiomics model can assist in the non-invasive preoperative prediction of the presence of STAS in the early stage of lung adenocarcinomas. The prediction model constructed with a combination of the Rad-score and conventional variables showed higher diagnostic performance for the presence of STAS than the conventional model in the multiple validation datasets.

According to previous studies regarding the conventional imaging features of STAS-positive non-small cell lung cancers, a larger tumor size and a high percentage of solid components on CT scans were associated with STAS-positivity,[15-18] which can be explained by the correlation with the histologic subtype. In surgically resected lung adenocarcinomas, tumors with STAS tended to be of more invasive histologic subtypes with a worse prognosis (e.g., solid or micropapillary predominance), while there were fewer tumors of the lepidic histologic subtype than those without STAS. Given that GGO in subsolid nodules is believed to correlate with the lepidic component of lung adenocarcinomas, lung adenocarcinomas with preinvasive or lepidic-predominant subtypes are mostly present as pure GGNs or PSNs on CT, whereas lung adenocarcinomas of micropapillary or solid-predominant subtypes are present as pure solid nodules.

In our study, the combined model (constructed with conventional variables and radiomics features) showed a higher AUC compared to the conventional model, indicating the added value of the radiomics model. Two selected radiomics features in our study are thought to have contributed to the model performance since STAS-positive lung adenocarcinomas have poor prognoses and are associated with aggressive tumor behavior,[43] which may implicate intratumoral heterogeneity or a poor peritumoral microenvironment. Although conventional CT parameters, such as lesion type and solid portion size, may also implicate those lesion characteristics, radiomics may provide the further information about the lesion heterogeneity. Indeed, the Rad-score for STAS prediction was significantly different between histologic subtypes in our study, in that the high-risk subtypes (solid or micropapillary) showed higher Rad-scores compared to other subtypes, which supports the association between the presence of STAS and histologic subtypes. Additionally, our Rad-score was not directly correlated with other pathologic or biologic variables, but its association with recurrence-free survival highlights the clinical implication of radiomics in the early stage of surgically resected lung adenocarcinomas.

Previous studies have investigated the value of radiomics features for STAS prediction, mostly in patients with early stage surgically resected lung adenocarcinoma.[23-29,44-48] Most previous studies constructed radiomics models using radiomics features, with the number of selected features ranging from 2 to

https://doi.org/10.3349/ymj.2023.0368

12, and reported the performance of the model using the AUC, which ranged from 0.63 to 0.99. Although all previous studies concluded that radiomics features were useful for the preoperative prediction of STAS, the actual added value of radiomics to the conventional prediction model and the association with survival were rarely investigated.[28,46] Moreover, most studies validated their radiomics models using internal validation datasets (cross-validation, or random split sample); therefore, external validation using datasets from other institutions were rarely performed.[26,29,45]

The strength of our study over previous studies lies mainly in the validation of the model using multiple datasets and pursuing the quality of science along with the radiomics quality score. The radiomics model for the prediction of STAS, which was developed using the dataset from one institution, showed added value to the conventional model in test and validation datasets from the same institution. Validation sets consisted of the internal validation dataset of heterogenous CT protocols that were acquired at the outside hospitals and the temporal validation dataset of different time periods. These results suggest that our radiomics model has internal validity and temporal generalizability, but does not reach geographic or domain generalizability.[49]

The performance of the radiomics model could be affected by the heterogeneity in CT parameters (e.g. contrast administration or reconstruction kernels) or variability within the population (e.g., differences in the proportion of STAS-positive tumors or CT lesion type) among datasets.[50] CT scanning parameters may affect the stability and reproducibility of radiomics features. However, we assumed that the effect of CT parameters was not critical to our results since our internal validation set, which consisted of heterogenous CT scans acquired with various CT scanners and protocols, showed a higher AUC for the combined model compared to the clinical model (0.878 vs. 0.854) for preoperative STAS prediction. This result is in line with that of a previous study which reported the performance of a radiomics model from a dataset showing heterogeneity with respect to CT manufacturer, machine type, or protocol.[44] Additionally, the AUCs of models were not significantly different when applying the combat method to compensate the effect of the contrast administration.

This study has several limitations that warrant discussion. First, since it was a retrospective study, an inherent selection bias is to be expected. Second, we performed semi-automatic segmentation of tumor, which can show variable results according to the reader. Especially, excluding the internal vessel or bronchiole can be difficult in cases of pure GGNs or PSN, and these can result in interobserver variability of the segmentation results, despite most of the radiomics features in our study showing good-to-excellent interobserver agreement. Third, since we validated the performance of conventional and combined models in the internal datasets that were acquired from multiple institutions and temporal datasets, the validation in a large number of external datasets would be needed to ensure the generalizability of our results. Fourth, the sensitivity of detection of STAS on pathology may vary among institutions as the identification of STAS is often challenging due to the development of ex-vivo artifacts that complicate interpretation.[51] Finally, applying the novel technique of image conversion of slice thickness or reconstruction kernel may be helpful to overcome the potential effect of CT protocols.[52,53]

In conclusion, quantitative CT radiomics features can help to predict the presence of STAS preoperatively in the early stage of lung adenocarcinomas. A combined model composed of conventional clinical and CT variables and CT radiomics features may have added value for non-invasive assessment of the presence of STAS in conventional models.

ACKNOWLEDGEMENTS

This work was supported by a faculty research grant of Yonsei University College of Medicine (6-2020-0209).

AUTHOR CONTRIBUTIONS

Conceptualization: Young Joo Suh. Data curation: Young Joo Suh, Sung Ho Hwang, Myung Hyun Kim, Hyun Joo Shin, Chang Young Lee, and Hyo Sup Shim. Formal analysis: Young Joo Suh, Kyunghwa Han, Yonghan Kwon, and Hwiyoung Kim. Funding acquisition: Young Joo Suh. Investigation: Young Joo Suh, Kyunghwa Han, and Suji Lee. Methodology: Young Joo Suh and Kyunghwa Han. Project administration: Young Joo Suh. Resources: Young Joo Suh. Software: Young Joo Suh. Supervision: Young Joo Suh and Kyunghwa Han. Validation: Young Joo Suh, Kyunghwa Han, Sung Ho Hwang, and Hyun Joo Shin. Visualization: Young Joo Suh, Kyunghwa Han, and Yonghan Kwon. Writing—original draft: Young Joo Suh. Writing—review & editing: all authors. Approval of final manuscript: all authors.

ORCID iDs

Young Joo Suh https://orcid.org/0000-0002-2078-5832
Kyunghwa Han https://orcid.org/0000-0002-5687-7237
Yonghan Kwon https://orcid.org/0000-0001-7951-1142
Hwiyoung Kim https://orcid.org/0000-0001-7778-8973
Suji Lee https://orcid.org/0000-0002-8770-622X
Sung Ho Hwang https://orcid.org/0000-0003-1850-0751
Myung Hyun Kim https://orcid.org/0000-0002-5139-0155
Hyun Joo Shin https://orcid.org/0000-0002-7462-2609
Chang Young Lee https://orcid.org/0000-0002-2404-9357
Hyo Sup Shim https://orcid.org/0000-0002-5718-3624

REFERENCES

1. Ferlay J, Soerjomataram I, Dikshit R, Eser S, Mathers C, Rebelo M, et al. Cancer incidence and mortality worldwide: sources, methods and major patterns in GLOBOCAN 2012. Int J Cancer 2015;136:E359-86.
2. Torre LA, Bray F, Siegel RL, Ferlay J, Lortet-Tieulent J, Jemal A. Global cancer statistics, 2012. CA Cancer J Clin 2015;65:87-108.
3. Warth A, Muley T, Meister M, Stenzinger A, Thomas M, Schirm-

acher P, et al. The novel histologic International Association for the Study of Lung Cancer/American Thoracic Society/European Respiratory Society classification system of lung adenocarcinoma is a stage-independent predictor of survival. J Clin Oncol 2012;30:1438-46.
4. Goldstraw P, Chansky K, Crowley J, Rami-Porta R, Asamura H, Eberhardt WE, et al. The IASLC lung cancer staging project: proposals for revision of the TNM stage groupings in the forthcoming (eighth) edition of the TNM classification for lung cancer. J Thorac Oncol 2016;11:39-51.
5. Gu J, Lu C, Guo J, Chen L, Chu Y, Ji Y, et al. Prognostic significance of the IASLC/ATS/ERS classification in Chinese patients—A single institution retrospective study of 292 lung adenocarcinoma. J Surg Oncol 2013;107:474-80.
6. Russell PA, Barnett SA, Walkiewicz M, Wainer Z, Conron M, Wright GM, et al. Correlation of mutation status and survival with predominant histologic subtype according to the new IASLC/ATS/ERS lung adenocarcinoma classification in stage III (N2) patients. J Thorac Oncol 2013;8:461-8.
7. Travis WD, Brambilla E, Nicholson AG, Yatabe Y, Austin JHM, Beasley MB, et al. The 2015 World Health Organization classification of lung tumors: impact of genetic, clinical and radiologic advances since the 2004 classification. J Thorac Oncol 2015;10:1243-60.
8. Kadota K, Nitadori JI, Sima CS, Ujiie H, Rizk NP, Jones DR, et al. Tumor spread through air spaces is an important pattern of invasion and impacts the frequency and location of recurrences after limited resection for small stage I lung adenocarcinomas. J Thorac Oncol 2015;10:806-14.
9. Shiono S, Yanagawa N. Spread through air spaces is a predictive factor of recurrence and a prognostic factor in stage I lung adenocarcinoma. Interact Cardiovasc Thorac Surg 2016;23:567-72.
10. Jia M, Yu S, Yu J, Li Y, Gao H, Sun PL. Comprehensive analysis of spread through air spaces in lung adenocarcinoma and squamous cell carcinoma using the 8th edition AJCC/UICC staging system. BMC Cancer 2020;20:705.
11. Yanagawa N, Shiono S, Endo M, Ogata SY. Tumor spread through air spaces is a useful predictor of recurrence and prognosis in stage I lung squamous cell carcinoma, but not in stage II and III. Lung Cancer 2018;120:14-21.
12. Eguchi T, Kameda K, Lu S, Bott MJ, Tan KS, Montecalvo J, et al. Lobectomy is associated with better outcomes than sublobar resection in spread through air spaces (STAS)-positive T1 lung adenocarcinoma: a propensity score–matched analysis. J Thorac Oncol 2019;14:87-98.
13. Morimoto J, Nakajima T, Suzuki H, Nagato K, Iwata T, Yoshida S, et al. Impact of free tumor clusters on prognosis after resection of pulmonary adenocarcinoma. J Thorac Cardiovasc Surg 2016;152:64-72.e1.
14. Walts AE, Marchevsky AM. Current evidence does not warrant frozen section evaluation for the presence of tumor spread through alveolar spaces. Arch Pathol Lab Med 2018;142:59-63.
15. Kim SK, Kim TJ, Chung MJ, Kim TS, Lee KS, Zo JI, et al. Lung adenocarcinoma: CT features associated with spread through air spaces. Radiology 2018;289:831-40.
16. de Margerie-Mellon C, Onken A, Heidinger BH, VanderLaan PA, Bankier AA. CT manifestations of tumor spread through airspaces in pulmonary adenocarcinomas presenting as subsolid nodules. J Thorac Imaging 2018;33:402-8.
17. Toyokawa G, Yamada Y, Tagawa T, Kamitani T, Yamasaki Y, Shimokawa M, et al. Computed tomography features of resected lung adenocarcinomas with spread through air spaces. J Thorac Cardiovasc Surg 2018;156:1670-6.e4.
18. Suh JW, Jeong YH, Cho A, Kim DJ, Chung KY, Shim HS, et al. Stepwise flowchart for decision making on sublobar resection through the estimation of spread through air space in early stage lung cancer(1). Lung Cancer 2020;142:28-33.
19. Jia TY, Xiong JF, Li XY, Yu W, Xu ZY, Cai XW, et al. Identifying EGFR mutations in lung adenocarcinoma by noninvasive imaging using radiomics features and random forest modeling. Eur Radiol 2019;29:4742-50.
20. Ozkan E, West A, Dedelow JA, Chu BF, Zhao W, Yildiz VO, et al. CT gray-level texture analysis as a quantitative imaging biomarker of epidermal growth factor receptor mutation status in adenocarcinoma of the lung. AJR Am J Roentgenol 2015;205:1016-25.
21. Liu Y, Kim J, Balagurunathan Y, Li Q, Garcia AL, Stringfield O, et al. Radiomic features are associated with EGFR mutation status in lung adenocarcinomas. Clin Lung Cancer 2016;17:441-8.e6.
22. Rizzo S, Petrella F, Buscarino V, De Maria F, Raimondi S, Barberis M, et al. CT radiogenomic characterization of EGFR, K-RAS, and ALK mutations in non-small cell lung cancer. Eur Radiol 2016;26:32-42.
23. Chetan MR, Gleeson FV. Radiomics in predicting treatment response in non-small-cell lung cancer: current status, challenges and future perspectives. Eur Radiol 2021;31:1049-58.
24. Zhuo Y, Feng M, Yang S, Zhou L, Ge D, Lu S, et al. Radiomics nomograms of tumors and peritumoral regions for the preoperative prediction of spread through air spaces in lung adenocarcinoma. Transl Oncol 2020;13:100820.
25. Jiang C, Luo Y, Yuan J, You S, Chen Z, Wu M, et al. CT-based radiomics and machine learning to predict spread through air space in lung adenocarcinoma. Eur Radiol 2020;30:4050-7.
26. Chen D, She Y, Wang T, Xie H, Li J, Jiang G, et al. Radiomics-based prediction for tumour spread through air spaces in stage I lung adenocarcinoma using machine learning. Eur J Cardiothorac Surg 2020;58:51-8.
27. Liao G, Huang L, Wu S, Zhang P, Xie D, Yao L, et al. Preoperative CT-based peritumoral and tumoral radiomic features prediction for tumor spread through air spaces in clinical stage I lung adenocarcinoma. Lung Cancer 2022;163:87-95.
28. Han X, Fan J, Zheng Y, Ding C, Zhang X, Zhang K, et al. The value of CT-based radiomics for predicting spread through air spaces in stage IA lung adenocarcinoma. Front Oncol 2022;12:757389.
29. Chen LW, Lin MW, Hsieh MS, Yang SM, Wang HJ, Chen YC, et al. Radiomic values from high-grade subtypes to predict spread through air spaces in lung adenocarcinoma. Ann Thorac Surg 2022;114:999-1006.
30. Lambin P, Leijenaar RTH, Deist TM, Peerlings J, de Jong EEC, van Timmeren J, et al. Radiomics: the bridge between medical imaging and personalized medicine. Nat Rev Clin Oncol 2017;14:749-62.
31. Park EA, Lee HJ, Kim YT, Kang CH, Kang KW, Jeon YK, et al. EGFR gene copy number in adenocarcinoma of the lung by FISH analysis: investigation of significantly related factors on CT, FDG-PET, and histopathology. Lung Cancer 2009;64:179-86.
32. Travis WD, Asamura H, Bankier AA, Beasley MB, Detterbeck F, Flieder DB, et al. The IASLC lung cancer staging project: proposals for coding T categories for subsolid nodules and assessment of tumor size in part-solid tumors in the forthcoming eighth edition of the TNM classification of lung cancer. J Thorac Oncol 2016;11:1204-23.
33. Bankier AA, MacMahon H, Goo JM, Rubin GD, Schaefer-Prokop CM, Naidich DP. Recommendations for measuring pulmonary nodules at CT: a statement from the Fleischner society. Radiology 2017;285:584-600.
34. van Griethuysen JJM, Fedorov A, Parmar C, Hosny A, Aucoin N, Narayan V, et al. Computational radiomics system to decode the radiographic phenotype. Cancer Res 2017;77:e104-7.

https://doi.org/10.3349/ymj.2023.0368

35. Zwanenburg A, Vallières M, Abdalah MA, Aerts HJWL, Andrearczyk V, Apte A, et al. The image biomarker standardization initiative: standardized quantitative radiomics for high-throughput image-based phenotyping. Radiology 2020;295:328-38.
36. Gaber R, Kameda K, Eguchi T, Tano Z, Jones D, Travis W, et al. MA 15.09 circumferential distribution and distance from main tumor of tumor spread through air spaces (STAS) are prognostic. J Thorac Oncol 2017;12(supplement 2):S1864.
37. Travis WD, Brambilla E, Noguchi M, Nicholson AG, Geisinger KR, Yatabe Y, et al. International Association for the Study of Lung Cancer/American Thoracic Society/European Respiratory Society international multidisciplinary classification of lung adenocarcinoma. J Thorac Oncol 2011;6:244-85.
38. Tibshirani R. Regression shrinkage and selection via the lasso. J R Stat Soc B Stat Methodol 1996;58:267-88.
39. Huang Y, Liu Z, He L, Chen X, Pan D, Ma Z, et al. Radiomics signature: a potential biomarker for the prediction of disease-free survival in early-stage (I or II) non—small cell lung cancer. Radiology 2016;281:947-57.
40. Orlhac F, Frouin F, Nioche C, Ayache N, Buvat I. Validation of a method to compensate multicenter effects affecting CT radiomics. Radiology 2019;291:53-9.
41. Johnson WE, Li C, Rabinovic A. Adjusting batch effects in microarray expression data using empirical Bayes methods. Biostatistics 2007;8:118-27.
42. DeLong ER, DeLong DM, Clarke-Pearson DL. Comparing the areas under two or more correlated receiver operating characteristic curves: a nonparametric approach. Biometrics 1988;44:837-45.
43. Lee JS, Kim EK, Kim M, Shim HS. Genetic and clinicopathologic characteristics of lung adenocarcinoma with tumor spread through air spaces. Lung Cancer 2018;123:121-6.
44. Bassi M, Russomando A, Vannucci J, Ciardiello A, Dolciami M, Ricci P, et al. Role of radiomics in predicting lung cancer spread through air spaces in a heterogeneous dataset. Transl Lung Cancer Res 2022;11:560-71.
45. Qi L, Li X, He L, Cheng G, Cai Y, Xue K, et al. Comparison of diagnostic performance of spread through airspaces of lung adenocarcinoma based on morphological analysis and perinodular and intranodular radiomic features on chest CT images. Front Oncol 2021;11:654413.
46. Onozato Y, Nakajima T, Yokota H, Morimoto J, Nishiyama A, Toyoda T, et al. Radiomics is feasible for prediction of spread through air spaces in patients with nonsmall cell lung cancer. Sci Rep 2021;11:13526.
47. Takehana K, Sakamoto R, Fujimoto K, Matsuo Y, Nakajima N, Yoshizawa A, et al. Peritumoral radiomics features on preoperative thin-slice CT images can predict the spread through air spaces of lung adenocarcinoma. Sci Rep 2022;12:10323.
48. Liu Q, Qi W, Wu Y, Zhou Y, Huang Z. Construction of pulmonary nodule CT radiomics random forest model based on artificial intelligence software for STAS evaluation of stage IA lung adenocarcinoma. Comput Math Methods Med 2022;2022:2173412.
49. de Hond AAH, Shah VB, Kant IMJ, Van Calster B, Steyerberg EW, Hernandez-Boussard T. Perspectives on validation of clinical predictive algorithms. NPJ Digit Med 2023;6:86.
50. Van Calster B, Steyerberg EW, Wynants L, van Smeden M. There is no such thing as a validated prediction model. BMC Med 2023;21:70.
51. Blaauwgeers H, Flieder D, Warth A, Harms A, Monkhorst K, Witte B, et al. A prospective study of loose tissue fragments in non–small cell lung cancer resection specimens: an alternative view to "spread through air spaces". Am J Surg Pathol 2017;41:1226-30.
52. Choe J, Lee SM, Do KH, Lee G, Lee JG, Lee SM, et al. Deep learning–based image conversion of CT reconstruction kernels improves radiomics reproducibility for pulmonary nodules or masses. Radiology 2019;292:365-73.
53. Park S, Lee SM, Do KH, Lee JG, Bae W, Park H, et al. Deep learning algorithm for reducing CT slice thickness: effect on reproducibility of radiomic features in lung cancer. Korean J Radiol 2019;20:1431-40.